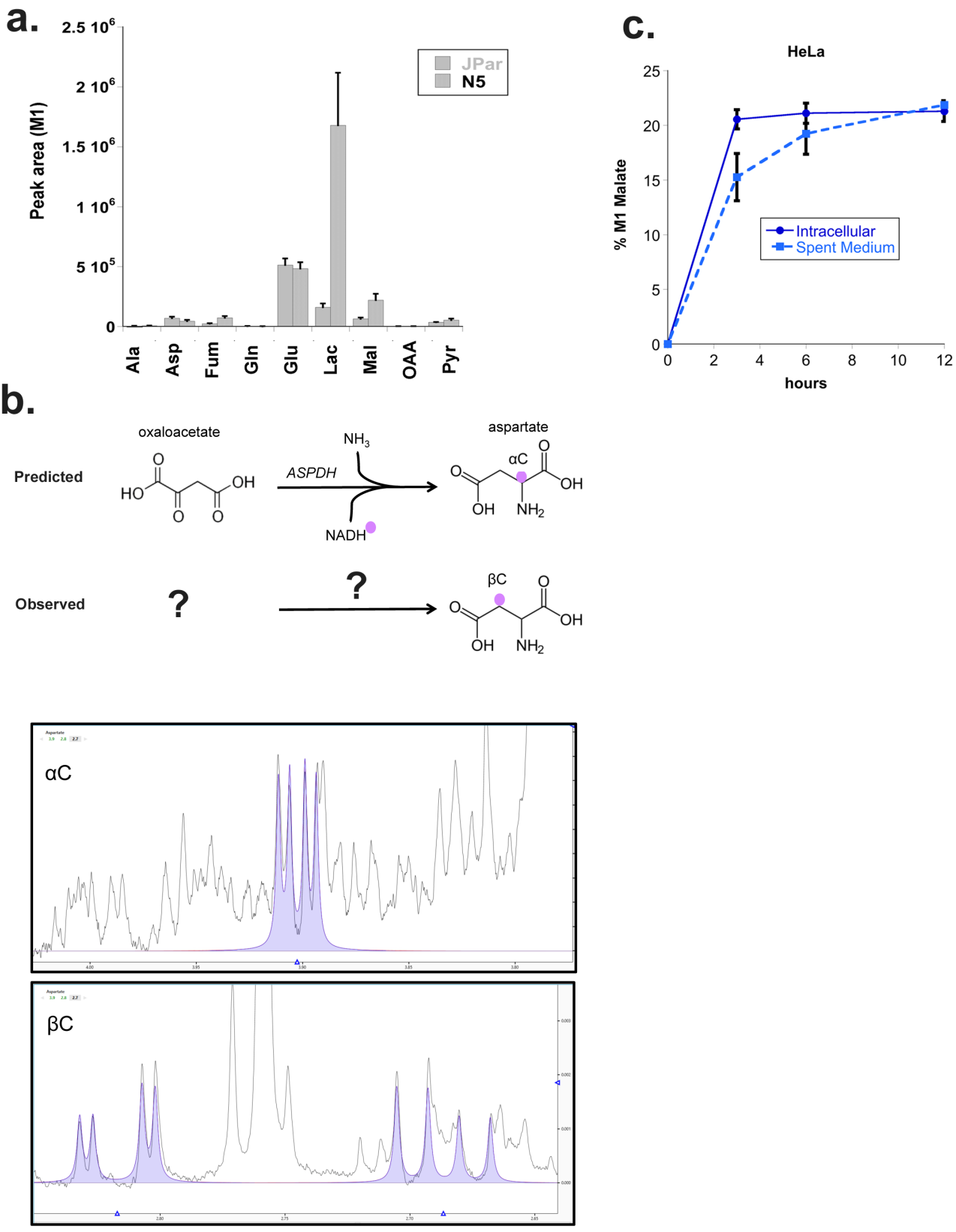

Supplementary Figure 1. (a) GC-MS peak values for the M1 measured metabolites indicated on the x-axis 24 hours after labeling with [4-^{2}H] glucose. (b) The aspartate dehydrogenase reaction as predicted by Yang et al in *Thermotoga maritima* and the aspartate labeling observed following [4-^{2}H] glucose labeling in N5 cells (top). NMR tracing for ^{1}H in the α and β carbon of aspartate following [4-^{2}H] glucose labeling. The partial depletion of ^{1}H on the β carbon indicates ^{2}H has replaced the ^{1}H. The aspartate reference peaks are shaded in blue (bottom). (c) Flux assay as in Figure 1D indicating M1 malate from [4-^{2}H] glucose within cells and expelled in the medium.

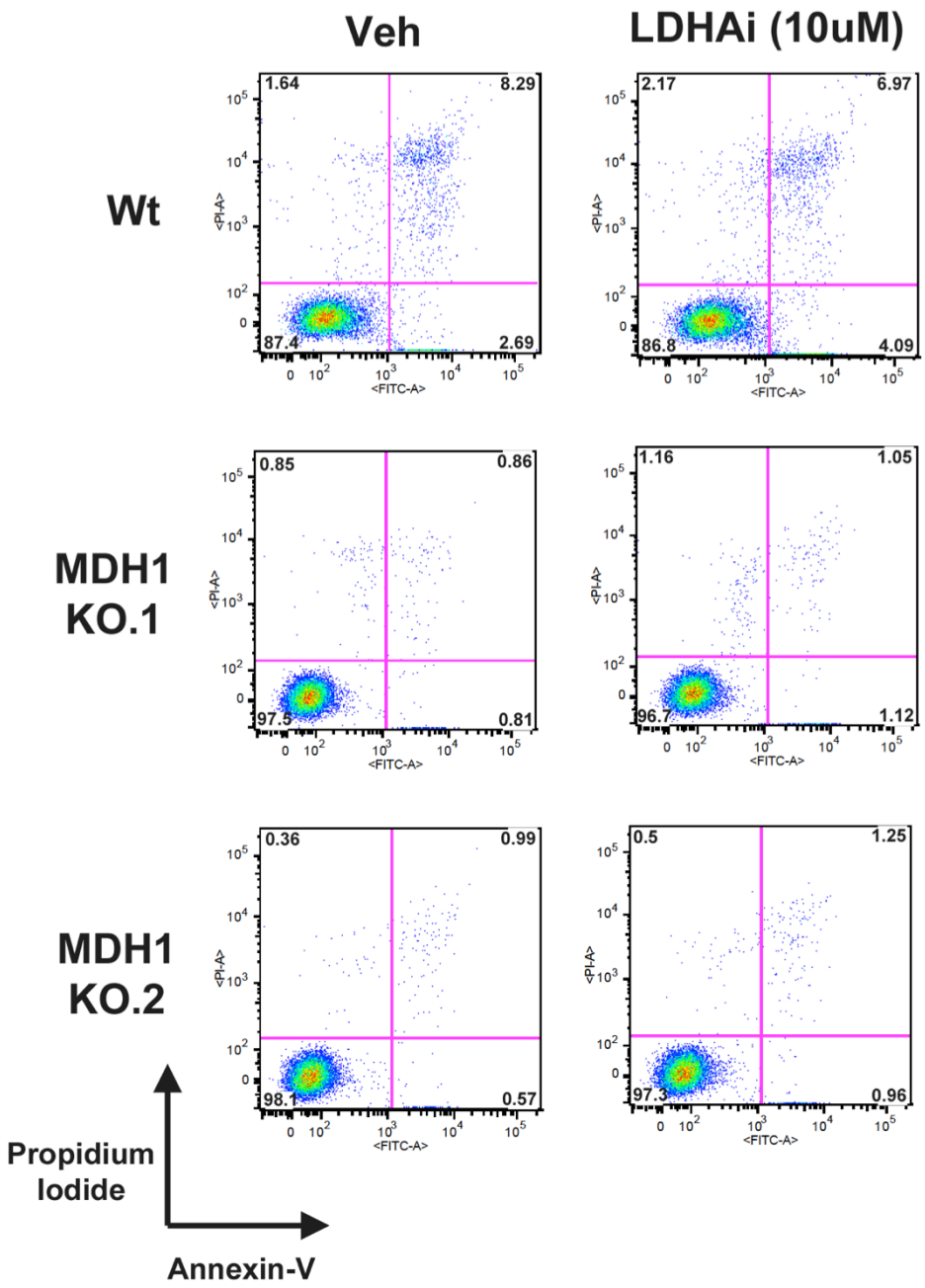

Supplementary Figure 2. Wt or MDH1 KO cells were treated with 10uM the of LDHA inhibitor GSK2837808A for 48 hours. Cells were collected, washed and stained with annexin-V-FITC and propidium iodide (PI). Cells were assessed for Annexin V-FITC/PI via flow cytometry using the LSR II (BD Bioscience). Data from 10,000 events were analyzed using the FlowJo Software Suite.

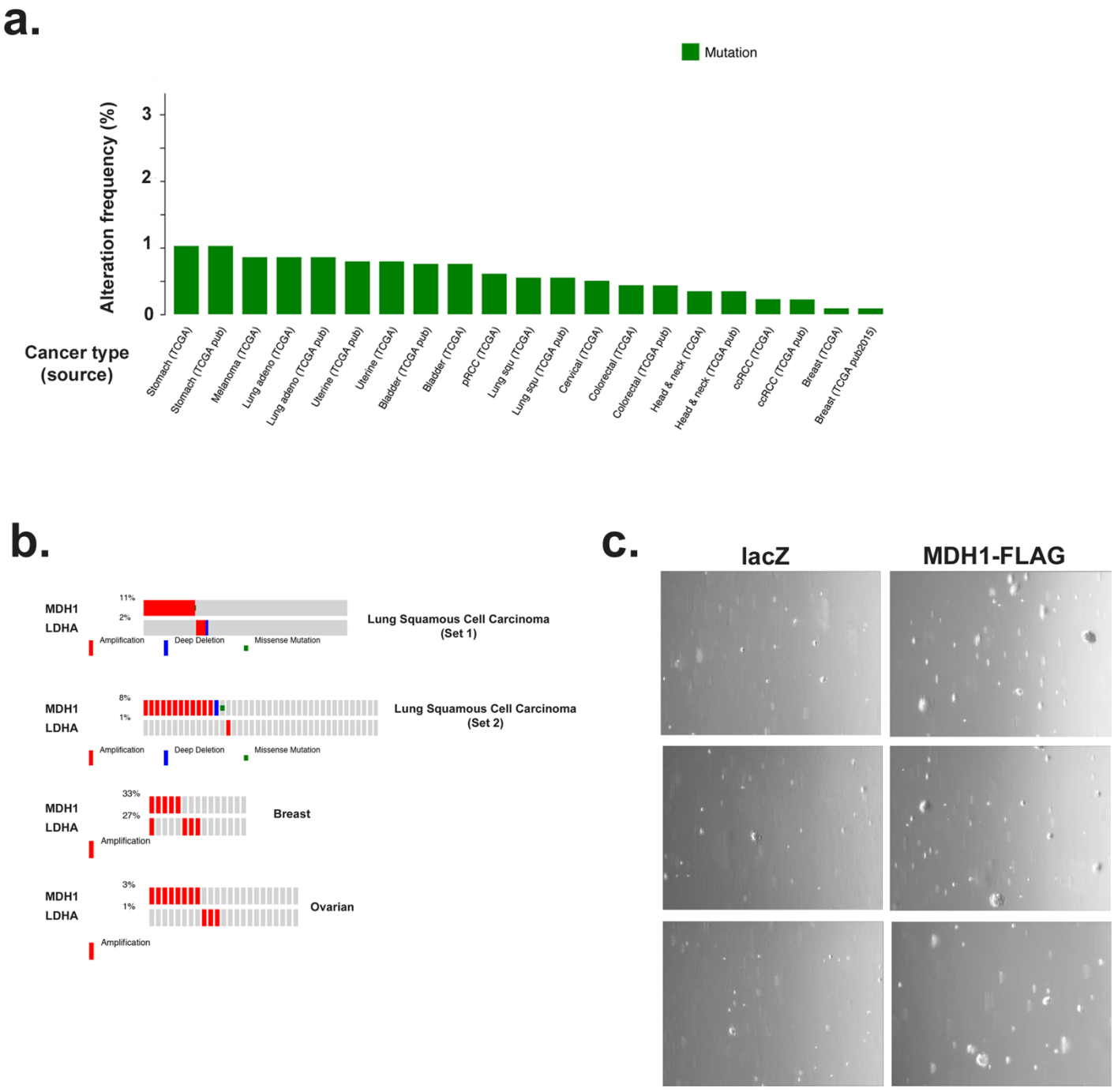

Supplementary Figure 3. (a) The Cancer Genome Atlas was accessed using the cBioportal. Percentage of MDH1 mutation was queried. Shown are the percentage of indicated tumor type with MDH1 mutation. Less than 1% of tumors contain mutated MDH1 suggesting the wild-type enzyme is preferred. (b) LDHA and MDH1 were cross-queried. Shown are genomic amplifications of MDH1 or LDHA from representative human tumor samples. Not all tumor samples are shown from each subset (denoted by gray bars) truncated representations are shown to highlight only those with genomic aberrations of MDH1 and LDHA. The percentages of genomic aberrations are indicated. (c) Representative low magnification phase contrast microscopy images of the soft agar assays quantified in Figure 4E.

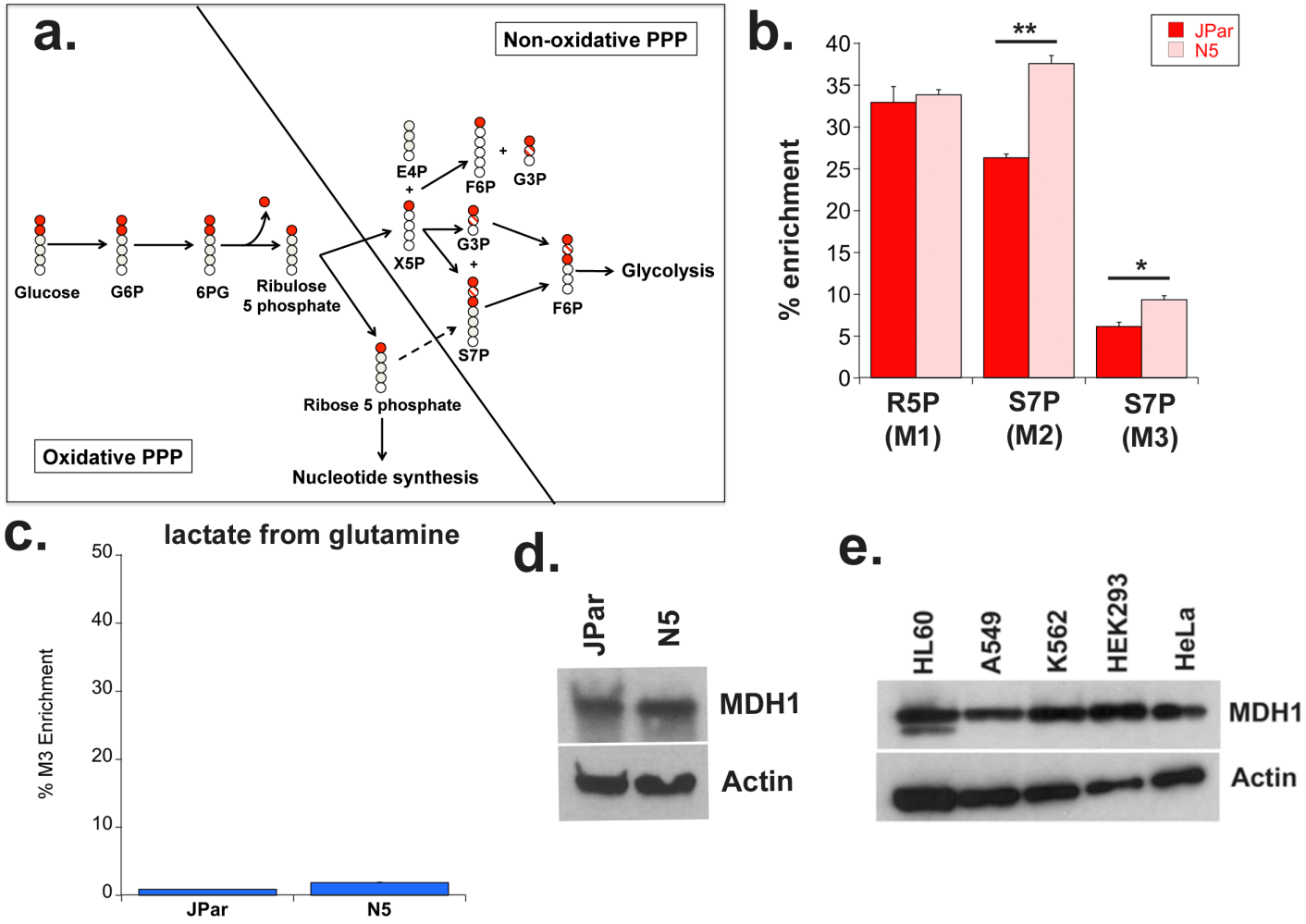

Supplementary Figure 4. (a) Simplified schematic diagram of the pentose phosphate pathway (PPP) tracing glucose carbons through portions of the oxidative and non-oxidative arm. (b) Noxa overexpressing cells increase glucose carbon flux to the non-oxidative phase of the pentose phosphate pathway. Experiments were performed as in Figure 4 using [1,2-^{13}C] D-glucose as a label. Shown is percent enrichment of M1 label from glucose into R5P and M2/M3 into S7P per the schematic in (a). R5P: ribose 5 phosphate/ribulose 5 phosphate (oxidative PPP metabolite). S7P: sedoheptulose 7 phosphate (non-oxidative PPP metabolite). (c) M3 lactate levels in cells fed with [U-^{13}C] glutamine as in Figure 6. Scale is indicated to compare to the lactate levels in Figure 6. Shown are the average and standard deviation of triplicate samples from a representative experiment repeated at least twice. Significance was calculated using the student's T test (* $p<0.01$, ** $p<0.001$). (d) Western blot comparing MDH1 expression between JPar and N5 cells. (e) Western blot comparing MDH1 expression between different cell lines.

Name	Method	Ion Quantified	Qualifier Ion (GC only)
SUC	LC-MS	117.019	n/a
G3P	LC-MS	168.99	n/a
2PG/3PG	LC-MS	184.986	n/a
CIT/ICIT	LC-MS	191.02	n/a
G6P	LC-MS	259.022	n/a
S7P	LC-MS	289.033	n/a
FBP	LC-MS	338.989	n/a
GLN	LC-MS	145.061	n/a
GLU	LC-MS	146.045	n/a
MAL	GC-MS	419.2	287.1
AKG	GC-MS	346.2	147.1
FUM	GC-MS	287.2	133.1
LAC	GC-MS	261.2	189.2
PYR	GC-MS	174.1	115.1

Supplementary Table 1. Ion Quantifiers and Ion Qualifiers used to identify metabolites in this study